63-2-4

FINAL REPORT
November 1962

CRACK INITIATION IN METALLIC MATERIALS

by

V. Weiss
K. Schroder
P. Packman and
J. G. Sessler

SYRACUSE UNIVERSITY RESEARCH INSTITUTE

DEPARTMENT OF CHEMICAL ENGINEERING AND METALLURGY
MET 878-6211-F

FINAL REPORT
November 1962

CRACK INITIATION IN METALLIC MATERIALS

by

V. Weiss
K. Schroder
P. Packman and
J. G. Sessler

SYRACUSE UNIVERSITY RESEARCH INSTITUTE

DEPARTMENT OF CHEMICAL ENGINEERING AND METALLURGY

Approved by:

Volker Weiss

S.U.R.I. Report No. MET. 878-6211-F

Sponsored by:

Department of the Navy
Bureau of Naval Weapons

Date: November 1962

TABLE OF CONTENTS

LIST OF TABLES

LIST OF FIGURES

INTRODUCTION

It was the purpose of the present investigation to study the parameters responsible for the initiation of fracture. This involves the determination of the stress or strain state under which an existing defect will spread and cause failure of the test piece. Thus, it is of importance to be concerned with both the creation of the defect in itself such as the formation of small cracks at the tip of machined notches or on the surface of smooth specimens as well as the propagation of these defects to failure. Depending on the outlook of the observer both phenomena could be termed as fracture initiation. An understanding of both phenomena, i.e. the formation of a crack on a smooth surface or at the root of a geometrically well defined notch as well as the propagation of an already existing crack is required in order to arrive at a basic understanding of fracture and thus bridge the gap between macroscopic and microscopic fracture concepts. The phenomenon of crack propagation per se, especially effects related to the kinetic energy dissipation during the propagation of a crack, was not considered in the present investigation.

Both energy balance as well as maximum stress concepts have been proposed for the initiation of brittle fracture[1]. The mathematical expressions of both concepts are almost identical. The differences between energy and stress approaches lie mostly in the physical interpretation of the mathematical symbols. Nevertheless, these philosphical differences are significant as guide lines for future research. One argument against the energy approach

1

is the statement that energy is a structure insensitive property while fracture certainly is a structure sensitive quantity. This argument is of course invalidated by the introduction of micro-mechanical energy concepts. However, the latter concepts have not yet been sufficiently developed while considerable experience both on a macroscopic as well as a microscopic scale is available concerning the interpretation of deformation phenomena on a stress analysis basis.

According to a maximum fracture stress concept [2] which is based on Neuber's theory of notch stresses, [3] fracture occurs when the stress in a given region exceeds a specified maximum value. This concept leads to an equation similar to that proposed by Griffith[4]. The concept is applicable to mild as well as sharp notches and can be easily amended for the case where plastic flow occurs, by means of a modified plasticity correction which was originally proposed by Hardrath and Ohman[5]. In addition, the effect of stress biaxiality developed at the root of a notch as a function of the thickness to root radius ratio, can be incorporated and a macroscopic interpretation of the degree of notch sensitivity is made possible by means of a plain strain notch ductility ratio[6].

Experimental results on brittle materials indicate that the notch strength ratio versus stress concentration factor curve trails off and becomes horizontal at a given stress concentration factor. This then indicates that additional sharpening of the notch root radius does not increase the stress concentration factor. The cause for this leveling off is mathematically explained by the introduction of an

equivalent particle size, which represents the limit of the applicability of continuum elasticity theory [2]. Estimates of this equivalent particle size η have yielded results in the order of .001 in. a size which should be readily observable by light microscopy techniques. It is evident that a physical interpretation of the meaning of this equivalent particle size would constitute significant progress towards bridging the gap between macroscopic and microscopic fracture concepts.

The present program consisted of an investigation of the conditions for crack initiation as a function of the test specimen geometry, the test material, the testing conditions and the internal structure of the material. Tungsten and titanium sheet specimens were selected for the studies. Lithium fluoride and silver chloride were utilized to yield information concerning the dislocation motion and arrangement at and near existing cracks.

The experimental results obtained to date are presented and discussed in this report, which summarizes the results of the first year's effort. These results include the study of the effects of recrystallization on the fracture strength of notched tungsten specimens, of the surface condition of smooth and notched titanium and tungsten specimens as well as a description of the dislocation arrangements in lithium fluoride single crystals near existing cracks. Tensile and notch tensile specimens containing both machined as well as fatigue cracked notches were utilized. Selected tungsten and titanium specimens were tested after the surface had been electropolished and the notch root had been prepared by electro-lytical machining. In this way very well defined test specimen surfaces

3

were used in the test program. An electrolytic saw which allowed the preparation of smooth notches without plastically deforming the surface and subsurface layers was constructed for this program. A number of furnaces have been constructed to allow proper recrystallization treatments of tungsten. A new test fixture was also constructed in order to insure fracture within the test section.

In addition to continuation of the present program the effects of material ductility on crack initiation will be studied. Other pure and well defined materials will also be inclused in next year's efforts.

THEORETICAL CONSIDERATIONS

A maximum fracture stress concept based on Neuber's theory of stress concentration [3] was originally proposed by Sachs, Weiss and Sessler[7, 8, 9]. In its most elementary form it states that

$$\sigma_N = \frac{\sigma_{max}}{K} \tag{1}$$

where σ_N is the net notched section stress, σ_{max} the fracture stress of an unnotched specimen and K the stress concentration factor. For the case of a brittle material, Neuber's elastic stress concentration factor K_t can be substituted. The elastic stress concentration factor for shallow eliptical notches in sheet specimen is given by

$$K_{t,s} = 1 + 2\sqrt{\frac{t}{r}} \tag{2}$$

where t in the notch depth and r the root radius[3]. Equation (2) does not apply to extremely sharp notches since it is based on continuum theory of elasticity. A correction, taking into accounts the non-integrability of the stress field equations near the root of a sharp notch of a region η yields

$$K_{t,s} = 1 + 2\sqrt{\frac{t}{r + 2\eta}} \tag{3}$$

which is in agreement with experimental results obtained on a brittle titanium alloy[8, 10]. The quantity η is termed "equivalent particle size" and appears to be a material characteristic. It's value can be determined from log σ_N vs. log K_t curves at high K_t values where the curve becomes horizontal.

Two additional ways of determining the value of η were developed in this study. Assuming very sharp $(r \rightarrow o)$ and shallow notches, η can be determined from graphs log t vs log $(NSR/(1-NSR))$ according to

$$\frac{NSR}{1-NSR} \sqrt{4t} = \sqrt{2\eta} \qquad (4)$$

where NSR is the notch strength ratio as defined by $\mathcal{E}_N / \mathcal{E}_{max}$.
The intercept of this curve for NSR = 0.5, NSR/(1-NSR) = 1, yields $\eta = 2t$

For the case of specimens for which the shallow notch approximation is no longer applicable a solution for η was also obtained provided that $\eta \ll a, \eta \ll t$. Assuming again $r \rightarrow o$, η is given by

$$\eta = \left(\frac{NSR}{1-NSR}\right)^2 \frac{1}{\frac{1}{2t} + \frac{\pi^2}{8a}} \qquad (5)$$

where 2a is the net section width of the test specimen.

A moderate amount of plastic flow can be accounted for by a plasticity correction proposed by Hardrath and Ohman[5]. Accordingly the corrected stress concentration factor is given by

$$K = K_t (1 - p) + p \qquad (6)$$

where p is termed the notch ductility ratio which appears to be related to the elongation or reduction in area of a smooth tensile specimen. The approach taken is similar to that adopted by Gerard[11] et al. and attempts to utilize the notch ductility ratio as a quality number for materials evaluation with respect to notch sensitivity[12].

A better insight into the stress state at the root of a notch is obtained by knowing the stress gradient at that location. Calculations

have yielded[13]

$$\frac{d\sigma_y}{dx}\bigg/_{\sigma_y = \sigma_{Max}} = \frac{2\sigma_{Max}}{r} \tag{7}$$

which defines the relative elastic stress gradient as

$$\frac{1}{\sigma_N} \frac{d\sigma_x}{dx}\bigg/_{\sigma_x = \sigma_{Max}} = \frac{2K_t}{r} = \gamma \tag{8}$$

Two important phenomena relate to this stress gradient, namely the size effect and the stress biaxiality at the notch root. From equations (7 and 8) it is evident that the stress gradient decreases with increasing section size in geometrically similar specimens (K_t = constant). Thus an increase in size leads to an increase in the volume at the highly stressed region near the notch root which in turn can explain the observed size effect in geometrically similar specimens.

An analogy to the stress biaxiality developed in smooth bend specimens leads to the conclusion that the thickness to root radius ratio in notch tensile specimens determines the stress biaxiality at the center of the notch root. Plane strain conditions will be reached as soon as $t/r \geq 10$, a result experimentally confirmed by Loetsch[14]. Under these conditions, $t/r \geq 10$, the stress in the thickness direction is one half of the stress in the longitudinal direction. This plane strain condition in turn affects the fracture ductility and consequently the notch ductility ratio, as shown by Weiss and Sessler[6].

All these effects caused by the geometrical configuration, namely stress concentration factor, stress gradient, stress biaxiality and the intrinsic material properties expressed by the values of η, σ_{Max}, and p

7

have to be taken into consideration in an evaluation of materials fracture characteristics. For the present study, which is an attempt to bridge the gap between microscopic and macroscopic concepts a detailed examination of the physical meaning of σ_{max} and η is being undertaken. The concept of a constant maximum fracture stress as well as a constant value of η leads to

$$\sigma_{N}\sqrt{\pi t} = \sigma_{Max}\sqrt{\frac{\pi \eta}{2}} = K_c \qquad (9)$$

for shallow cracks, where K_c is the critical stress intensity factor which is in agreement with the energy concept of fracture proposed by Griffith[4] and Irwin[15].

EXPERIMENTAL RESULTS

FRACTURE OF Ti-2.5 Al-16V

Earlier investigations by Sachs and Sessler[10] showed that a titanium alloy Ti-2.5Al-16V can be heat treated to exhibit brittle fracture at room temperature. Their measurements indicate agreement with

$$\sigma_{max} = K_t \epsilon_N = \text{constant up to } K_t \approx 10.$$ One would therefore expect from equation 3 that the value of η to be of the order of 0.001 in. An attempt to determine a more precise value of η was undertaken on the same material. The specimen was provided with fatigue cracks in the solution treated condition and subsequently aged to an extremely brittle condition at 700 for 4 hours and furnace cooled. The specimen is illustrated in Figure 1. Figure 2 gives a presentation of the experimental data in accordance with equation 4 as $\log \dfrac{NSR}{1-NSR}$ versus $\log t$. Unfortunately the notch depth range covered is not sufficient for an accurate extrapolation of these data to $NSR/(1-NSR)=1$. The average value of η is approximately 0.003 in. Data on the same alloy obtained earlier from specimens provided with machined notches with a radius was 0.001 in. extrapolated to an η value of approximately 0.00056 in. However, these experiments cannot be compared with the present ones because a different heat of material and aging treatment was used. Experimental data from the present heat are also available for various root radii and a notch depth of 30%. Accordingly the intercept of the straight lines through these points having a slope -1/2 with $NSR/(1-NSR)=1$ should have values of $\eta + r_0/2$.

Table 1 lists the predicted values of $\eta + r_0/2$ in comparison with the observed values which are based on η equal to 0.003 in. It can be seen that the observed data appear to be in better agreement with the theoretical stress concentration factor if one uses not Neuber's equation (3) but an equation of the form

$$K \simeq 2 \sqrt{\frac{t}{r_0 + \eta}}$$

There exist at the moment no theoretical foundation for using this equation. Also, it should be pointed out that the tip of a natural crack is probably not representative of the properties of the undisturbed bulk of the material. The determination of η in accordance with equation (5) (finite geometry) is given in Table II. It should be noted that equation (5) is only valid for $r_0 = 0$, since only the first two terms of an expansion of $\arctan \sqrt{\frac{\alpha}{2\eta}}$ were used. If these and the above simplifications are not made, equations of third or fourth order in η result.

The results in Table II give an average value of η = 0.00152 in. The variations in η range from 0.0012 to 0.00176 in. Based on these results, it appears that values of η calculated from equation (5) are more nearly constant than those obtained by means of the shallow notch equation, (2). This should not be surprising since the use of shallow notch equations for notches between 15 and 50% is hardly justifiable.

One of the difficulties in experimental programs involving edge-cracked specimens is the eccentricity of loading due to unequal crack length. However, this can be accounted for by calculating the

additional bending moment resulting from eccentricity. A preliminary
check of this effect indicates that the error due to eccentricity is
at most 6% in terms of the notch strength values reported for the
present series.

It was decided to cut notches with an electrolytic saw in
order to eliminate all effects of machining, which could work harden
the surface and produce microcracks.

It has been realized that electropolishing is probably one of
the best methods to produce a really clean surface. Only sputtering in
an inert atmosphere seems to be able to produce an even better surface.
Because the stress measurements are carried out in standard equipment,
it seems to be futile to try tests with sputtered material. Therefore
it was decided to construct an electrolytic saw. The design followed
closely the suggestions made by Metzger[16].

A sketch of the saw is given in Figure 3. The specimen is
kept in a movable specimen holder and pushed against a wire which is
oscillated by a motor. This wire is the cathode, the specimen is the
anode. The electrolyte drops continuously on wire and specimen. A
voltage of 20 to 40 volts is applied to the system and surface
material is removed. Hence a shallow notch is cut into the specimen
with a speed of several thousands of an inch per hour.

The wire had a radius of approximately 0.001 in. Metzger
found that the radius of the notch root would be approximately twice
the radius of the wire, but micrographs indicated that the radius
obtained in these experiments was of the order 0.004 to 0.005 in.

It was not possible to produce a uniform notch but the surface of the notch seemed to be of high quality. Table III gives the result of tensile tests of notch specimens with a nominal composition of Ti-2.5Al-16V aged for 4 hours at 700 degrees in air and furnace cooled.

Table IV gives calculated stress concentration factors for these electrolytically notched specimens. The stress concentration was calculated using Neuber's shallow notch equation (equation 2) on the assumption that the radius was either 0.002 in. or 0.005 in. The first value of 0.002 in. was selected following Metzger's suggestion [16], the second radius seems to be more appropriate from micrographical evidence. Figure 4 shows the results in terms of σ_N vs K_t. The extrapolated ultimate fracture stress σ_{max} would be about 650 ksi if one assumes a radius of 0.005 in. This is much higher than the value of 200 ksi reported previously by Sachs and Sessler [2]. In spite of the fact that the results were obtained from a different heat, possible chemical variations do not seem sufficient to explain an increase of the extrapolated ultimate fracture stress by a factor of more than 3. It is believed that this increase in strength is due to a different state of the material at the surface of the notch. It has been mentioned before that machining produces a highly deformed surface layer with numerous scratches and grooves. It is difficult to predict what happens to this surface layer in detail during aging at 700°F. One would expect that some of the residual stress will be released but it is doubtful that all surface defects will be removed. Also, it is not possible that scratches will be removed at this temperature.

12

A detailed analysis of the effect of surface scratches produced by machining is given in the Appendix. There it is shown how the surface scratches cause additional stress concentrations and increase the geometrical stress concentration factor in a multiplicative way. The log σ versus log K_t cuve for electropolished specimens is moved by a factor of about 3 compared with the corresponding curves found for machined notches. Therefore one should associate a K_t factor of about 3 with surface scratches of the machined specimen.

BRITTLE FRACTURE OF TUNGSTEN

The metallurgical structure of titanium alloys, mentioned in the previous paragraph, is rather complicated. No detailed analysis of the phases of this alloy have been given, but it is likely that quite complicated transformations take place. The $\alpha-\beta$ transformation can take place and the formation of the ω phase is likely. This makes it practically impossible to analyse the results mentioned above in terms of a specific dislocation and point defect model. Only a material in which the defect structure, e.g. density of dislocation, impurity concentration, etc. is better known should give enough information to make an analysis possible. It was therefore decided to conduct similar experiments with tungsten specimens. Initial tests with tungsten specimens showed that a specimen form used previously, (Figure 5a) is not suitable for a very hard and brittle material. For instance it was found that it is very difficult to drill holes with high quality finish into tungsten. Small cracks are usually

produced during machining which caused the specimens to fail in the holes.

A new specimen and specimen grip design was adopted which eliminated the need for holes and minimized waste material. Figure 5 b gives the design of specimen and specimen holder. Photostatic studies showed that the contact area of the specimen with the specimen holder is highly stressed. These stresses are predominantly compressive. Smooth brittle specimens always failed in the area where the test section of the specimen widened for the shoulders. The stress concentration factor associated with this widened is of the order of 1.2. Thus it should be possible to test notches with a K_t value larger than 1.5. However, since the ultimate fracture stress of the material at an electrolytically cut notch is usually higher than at the machined surface, a higher value of K is generally required to insure fracture at the notch root. Only if it is possible to electropolish the whole specimen so that the ultimate fracture strength is the same all over the specimen one could use stress concentration factors below 2. Initial tests with titanium alloys showed that this specimen and specimen-holder design operated satisfactorily from room temperature to about 600°F. The shims used in the specimen-holder softened at high temperatures. Hardened tool steel shims will be used for higher temperatures.

Experimental results of tests on tungsten specimens are given in Figure 6 and 7. The values used for the calculation and the dimensions of the specimens are given in Table IV. Specimens of the following type have been used.

14

a. Tungsten as received, notches produced by machining

b. Tungsten as received, notches produced with the electrolytic saw

c. Tungsten re-crystallized, notches produced with the electrolytic saw

The specimens were tested either at room temperature or in a liquid nitrogen bath. It is surprising to note that the value of σ_N found for specimens tested in liquid nitrogen in the as received condition and specimens re-crystallized and tested at room temperature are one line on the log σ versus log K curve. This curve actually is the only one which intercepts the abscissa under 45° as predicted by Neuber's theory. The fracture values are also the lowest found in tests with tungsten. Highest fracture stress has been found for specimens in the as-received condition, notched electrolytically and tested at room temperature. It should be pointed out that a connecting line of these values are on a straight line in the log σ versus log K curve but this line does not intercept the abscissa under 45°.

An analysis of the plasticity factor (p), (Equation 6) following Hardrath and Ohman[5], utilizing graphs as given by Weiss[2], result in p = 0.6 for room temperature tested electrolytically notched tungsten, p = 0.5 room temperature tested, machined specimen and p = 0.05 for liquid nitrogen tested specimens.

Microscopic investigations showed that the surface of these electrolytically polished specimens showed a micro-structure, indicating some small plastic deformation. Further studies are necessary to show qualitatively the advent of deformation. There exists evidence that

tungsten single crystals deformed plastically at room temperature
provided that the surface is clean. This usually is achieved by removing
electrolytically more than 0.005 in. of surface material. It can be seen
in Figure 6 that the curves of electropolished and machined notched
specimens tested at room temperature do not differ greatly. This may
be due to plastic deformation of the surface of the electropolished
specimen producing, for instance, slip steps which can be associated
with stress concentrations (see Appendix). Figure 7 gives a plot of
log $\hat{\sigma}_G$ versus log t (t = depth of notch) as found for specimens with
electrolytically cut shallow notches. Griffith's theory predicts that
in the case of brittle fracture all points have to lie on a straight
line, which has a slope of - 1/2. Figure 7 shows this is experimentally
observed for both the room temperature and liquid nitrogen electrolytically
cut notches.

DISLOCATION STUDIES

It is realized that a final analysis of fracture has to be given
in a model of the defect structure of the material. Specifically it is
believed that fracture has to be explained in a model in which dislocation
movement plays a dominant part. Unfortunately, the dislocation densities
in metals are usually of the order of 10^8 to 10^{12} cm^{-2} so that it is not
possible to detect dislocations with optical microscopes. Only the use
of the electron microscope or field emission microscope will give in-
formation on the movement of dislocation in metals, and their interaction
with other defects such as vacancies, impurities atoms, etc. It was
therefore decided to make a series of experiments with lithium fluoride

16

and silver chloride where dislocation densities are several orders of magnitude below of those in metals.

In silver chloride it is possible to see dislocations in the interior of the material. Extreme care is required in the preparation of silver chloride crystals. Exposure to light precipitates groups of silver atoms destroying the uniformity of the crystals. All cutting and notching operations were carried out only under a dark room safety light or in a dark room. Attempts were made to move the dislocation revealed by etching with an applied external stress field. No detectable motion could be seen. It is likely that the procedure which makes it possible to see dislocation acts at the same time as pinning mechanism[17]. A typical array of dislocation in silver chloride single crystals is given in Figure 8.

Experiments with lithium fluoride are more promising because it is possible to test specimens easily in the brittle or in the ductile condition. Also, it is easier to make the dislocations visible on the surface. Lithium fluoride is usually ductile at room temperature but it can be embrittled with hydrogen. Fracture at liquid nitrogen temperature is always brittle. One disadvantage working with lithium fluoride is that it cleaves only on (100) surfaces. Therefore, it is not possible to orient crystals in such a way that the stress direction can be easily varied. Extensive work on etchpit patterns have been carried out by Gilman and Johnston[18,19,20]. Many of the polishing and etching procedures were obtained from their papers. The steps used in preparation of a lithium fluoride dislocation etch is as follows:

17

1) Polishing, one minute in concentrated HF

2) Rinse in acetone

3) Polish 3 to 5 minutes in 2 volume % solution of NH_4OH (vigorous agitation). Thus results were obtained using a final etch, consisting of a dilute aqueous solution of Fe F_3 (one minute vigorous agitation) (Etch W). Figure 9 gives a typical section of a (100) plane of cleaved LiF showing the high dislocation density. Future tests will be conducted with annealed crystals to produce a lower dislocation density.

Cleavage cracks were introduced in the LiF specimens by pressing with a sharp pin. The specimens were then etched in equal parts HF and acetic acid   saturated with FeF_3 to determine the dislocation arrays. Figure 10 shows the typical dislocation pattern. There are three faint dislocation lines emanating from the tip of the crack in (110) directions. Figure 11 shows the same area re-etched in Etch W to determine the full dislocation pattern.

Because it is possible to see individual dislocations in these crystals, it is hoped that it will be possible to study the correlation between η and dislocation distributions.

SUMMARY

As a result of this first year's effort the following concepts concerning θ_{max} and η were developed.

1) Polycrystalline tungsten sheet allows the use of a maximum fracture stress concept at $-320°F$ in all and at room temperature in the recrystallized condition. A small amount of plasticity is indicated at room temperature in the as-received condition

2) The maximum stress in nearly perfect brittle materials appears limited to values below the theoretical strength of $0.1E$ due to dislocation steps at the surface. This concept has been developed by Dr. Schroder and is presented in detail in Appendix I.

3) An additional limitation on the extrapolated maximum stress for brittle fracture is imposed by the surface condition of the notch. Superimposed stress concentrations may be caused by machining or other operations.

4) The physical significance of η is not yet clear but it may be related to the non-multiplicative effect of superimposed stress fields due to stress raisers.

5) It appears that there is a connection between the super-imposed stress field interpretation and a statistical approach,[21] the former being considerably more lucid with respect to physical interpretation.

19

TABLE I

Comparison of Predicted and Observed Values of $\eta + r_0/2$ for Various r_0 and Constant Notch Depth of 30 Percent Based on $\eta = 0.003$

r_0	$\eta + r_0/2$ predicted	$\eta + r_0/2$ observed	$\eta + r_0$ predicted
0	--	0.003	0.003
0.0007	0.00335	0.0034	0.0037
0.001	0.0035	0.0048	0.004
0.004	0.005	0.008	0.007
0.010	0.008	0.0138	0.013
0.025	0.0155	0.030	0.028

Note: All tests were performed on 0.090 in Ti-2.5Al-16V sheet aged at 700F, 4 hours.

20

TABLE II

Determination of η Using Combined Shallow and Deep Notch Equation

$$\eta = \left(\frac{\sigma_N}{F_{tu} - \sigma_N}\right)^2 \cdot \frac{1}{\frac{1}{2t} + \frac{\eta'^2}{8a}}$$

Spec.	σ_N	$\left(\dfrac{\sigma_N}{F_{tu} - \sigma_N}\right)^2$	$\dfrac{1}{\frac{1}{2t} + \frac{\eta'^2}{8a}}$	t (Average)	η in. x 10^3
F11	20.94	0.01366	0.109	0.0802	1.488
F16	19.31	0.01143	0.1093	0.0805	1.249
F13	20.51	0.01306	0.1319	0.1140	1.723
F14	20.96	0.01317	0.127	0.1053	1.740
F15	20.12	0.01252	0.141	0.1345	1.765
F12	17.84	0.00958	0.1387	0.1285	1.329
F18	19.11	0.01115	0.1507	0.2097	1.680
F19	16.71	0.00832	0.1409	0.2623	1.173

Note: F_{tu} determined to be 200 ksi by extrapolation

TABLE III

TITANIUM ALLOY TEST DATA

Specimen	Thickness (W)in	Width (D)in	Load lbs	Notch Depth (t)in	σ_G ksi	σ_N ksi	K_t (r = 0.002")	K_t (r = 0.005")
B3	.0649	.2498	1905	.035	117.6	162.8	6.65	4.32
B4	.0656	.2505	2180	.018	132.8	155.0	5.94	3.96
B5	.0637	.2500	2400	.016	150.8	171.8	5.74	3.87
B6	.0650	.2495	3190	.005	198.2	205.0	4.20	2.90

σ_G is equal to load/cross section of unnotched part of specimen (gross section stress) and

σ_N is equal to load/cross section between notches (notch stress of net section stress).

TABLE IV

TUNGSTEN TEST DATA

Specimen	Thickness (T)in	Width (W)in	Notch Depth (t)in	Root Radius in	Stress Conc K_t	Load (P) lbs	σ_G ksi	σ_N ksi
B1.5	.0497	.2415	—	.034	1.5	1500	125.8	170
B10	.0532	.0488	.010	.003	1.5	1060	80.3	87.1
B15	.0593	.2488	.017	.003	5.3	980	66.4	77.3
B20	.0528	.2468	.021	.003	5.9	800	61.2	74.2
B30	.0472	.2405	.037	.004	7.1	522	46.0	66.8
B40	.0578	.2445	.048	.004	7.8	510	36.1	59.6
*N10	.066	.2510	.012	.003	~4	490	32.5	36.0
N25	.0587	.2512	.024	.003	~6	357	29.5	23.8
N40	.0592	.2478	.044	.003	~6	190	12.9	20.0
**XR15	.0578	.2448	.015	.003	5.4	395	26.2	29.9
XR30	.0502	.2505	.030	.003	7.0	210	17.2	22.6

* N (Tested in Nitrogen)

**XR (Recrys. Room Temp Tested)

23

CRACK

2a

NOTCH OF 0.001 ROOT RADIUS,
0.050 DEEP

t

1.00

t = 0.075, 0.100, 0.150,
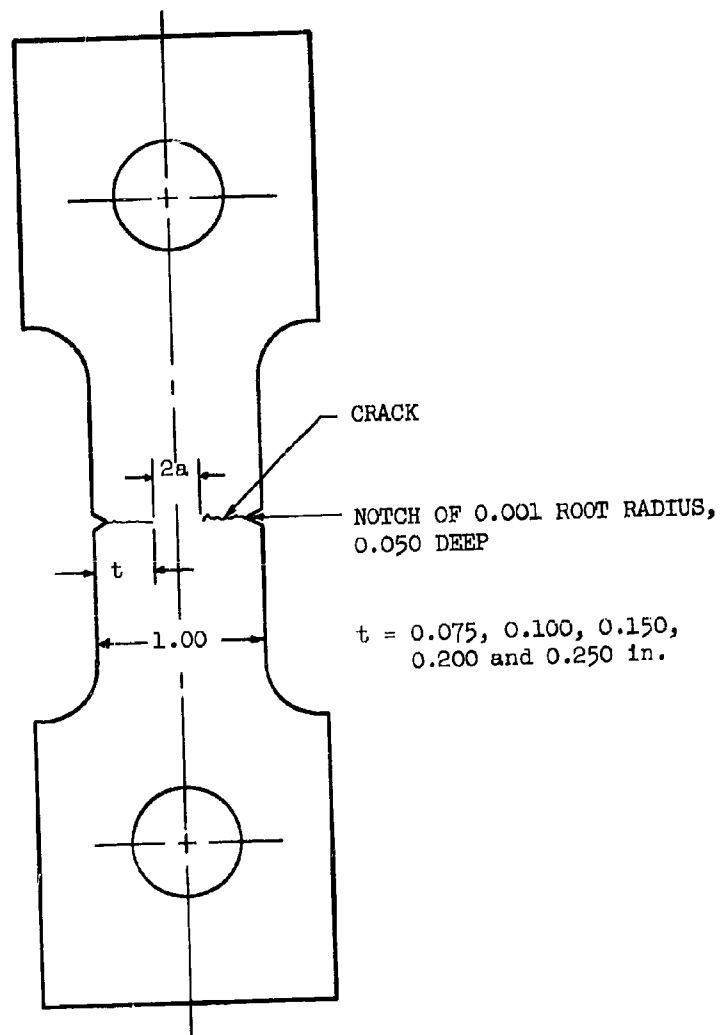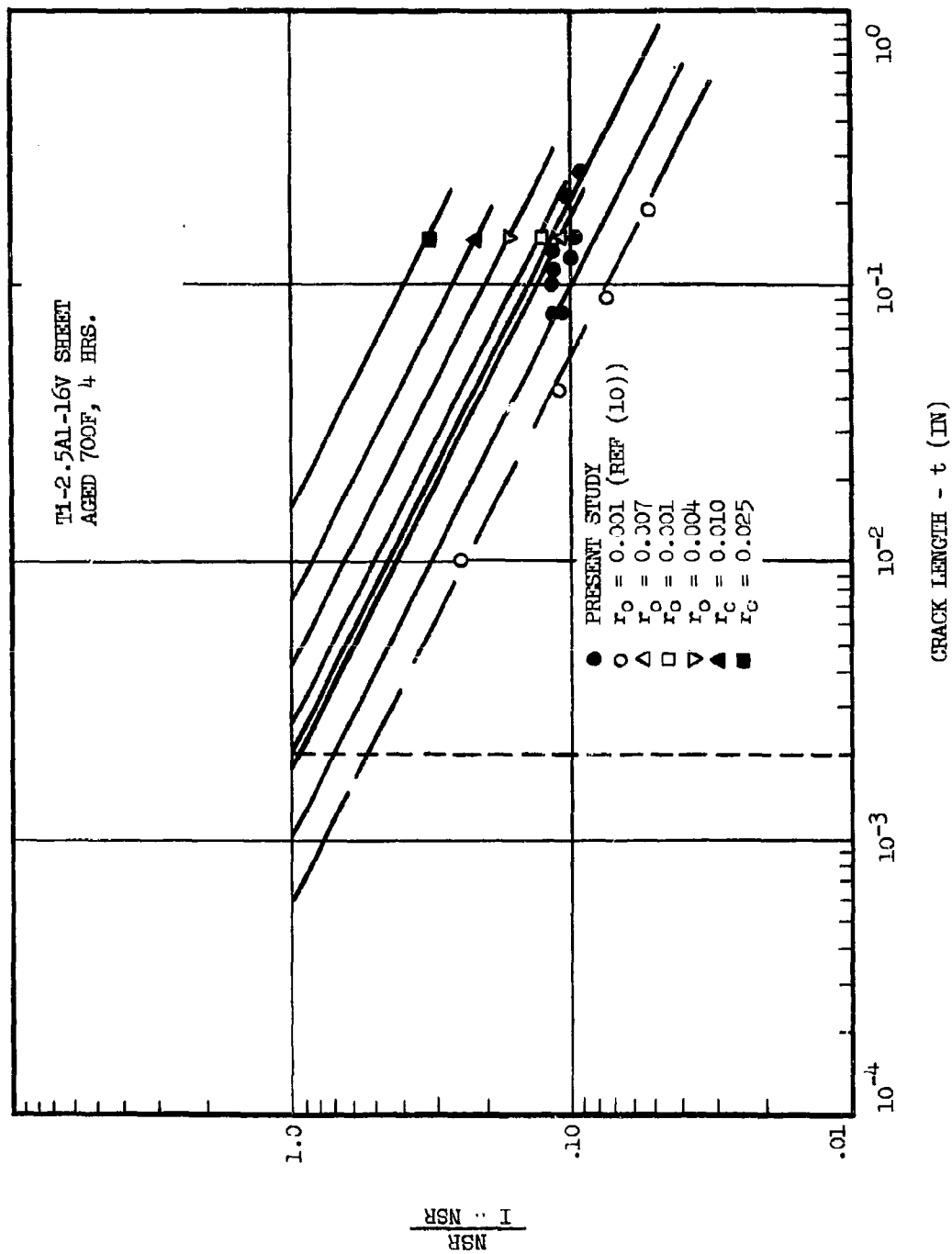0.200 and 0.250 in.

FIG. 1   CRACKED SPECIMEN

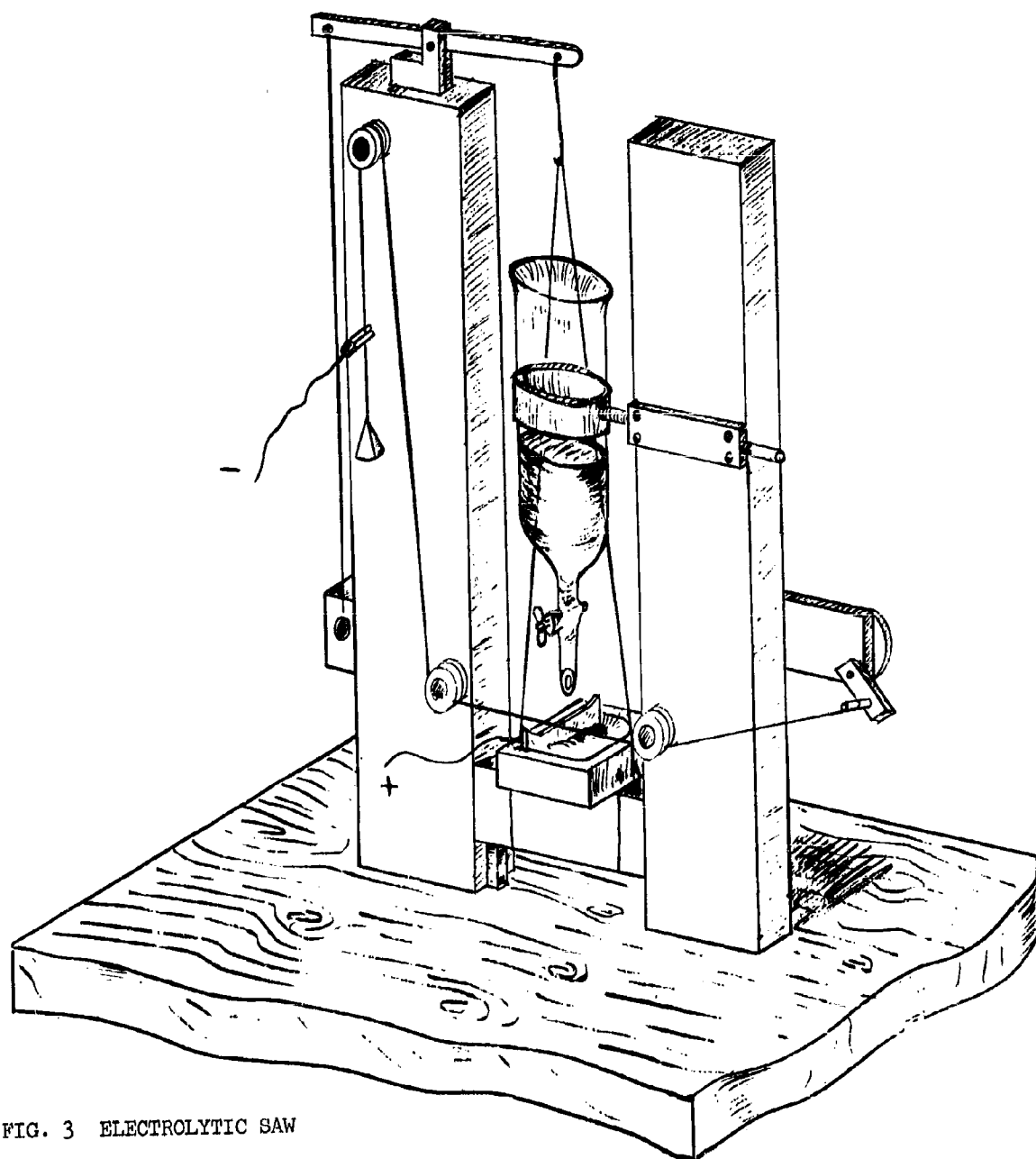FIG. 2 DETERMINATION OF η FROM EQUATION (4)
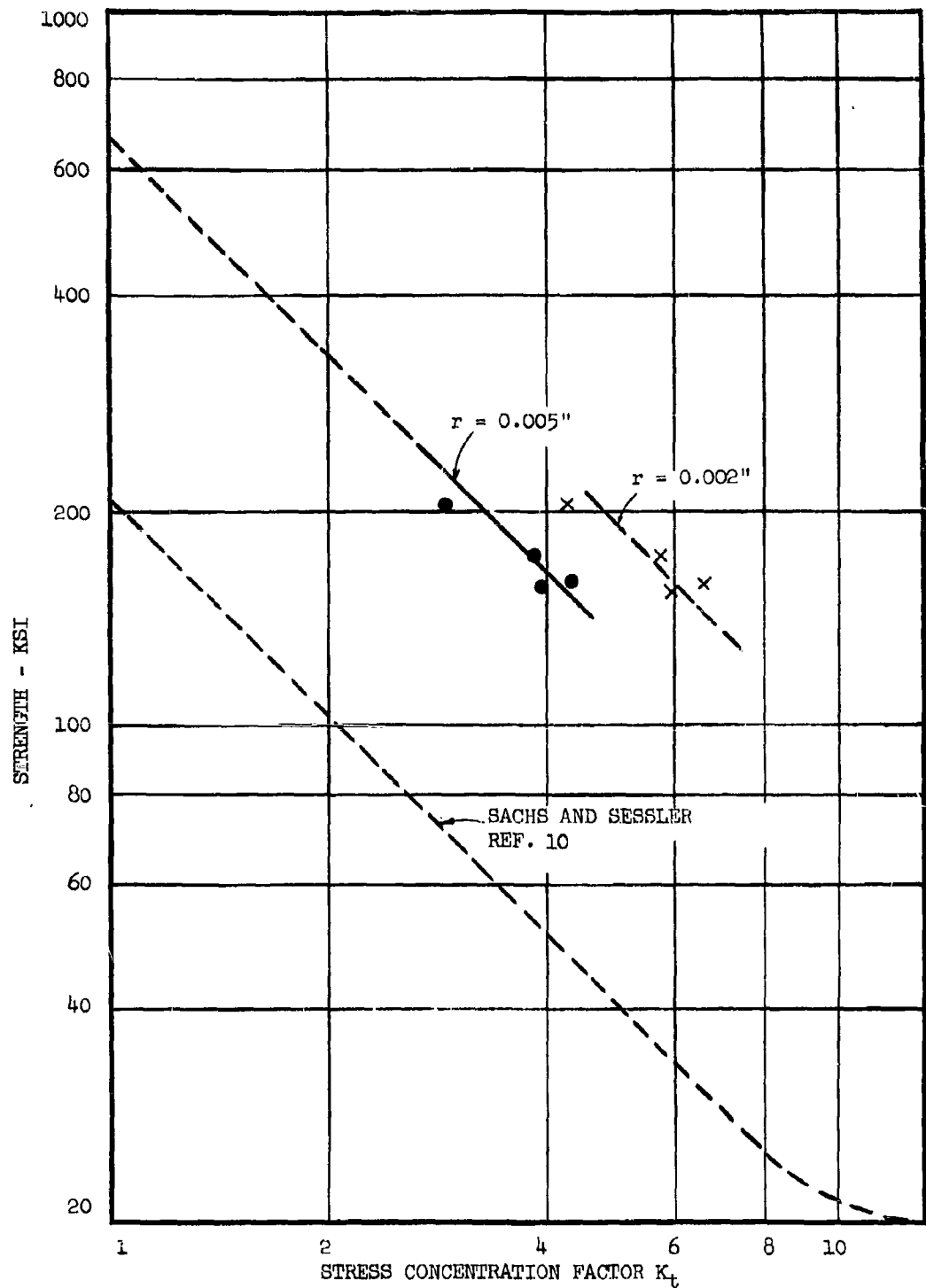
25

FIG. 3 ELECTROLYTIC SAW

FIG. 4 NOTCH STRENGTH VERSUS STRESS CONCENTRATION FACTOR OF Ti-2.5Al-16V, HEAT TREATED FOR MAXIMUM BRITTLENESS. NOTCHES PRODUCED WITH AN ELECTROLYTIC SAW.

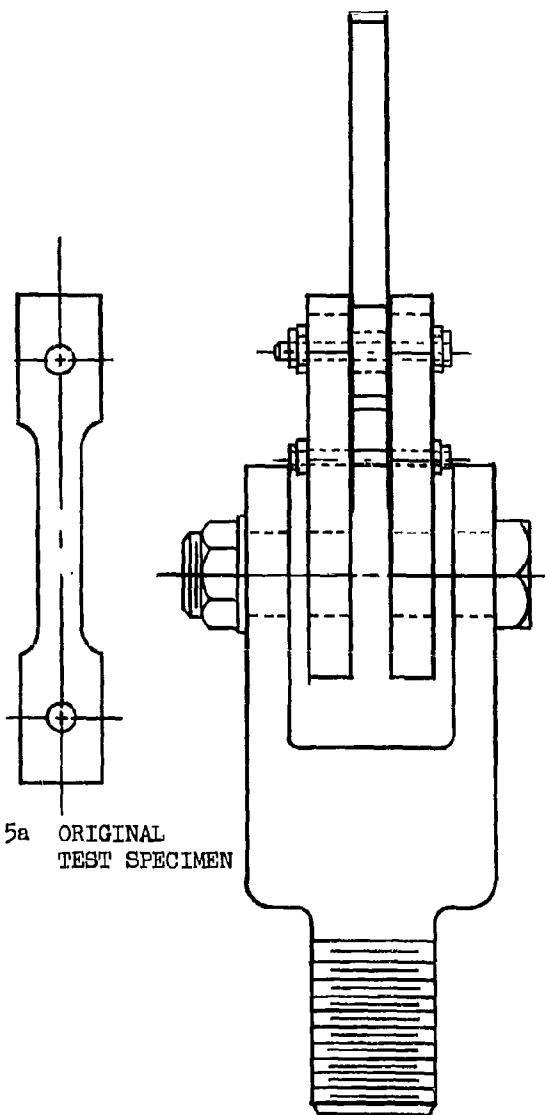FIG. 5a   ORIGINAL
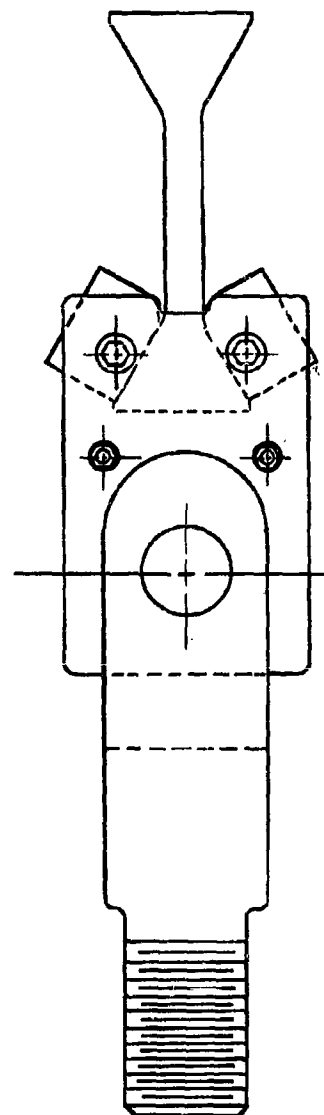   TEST SPECIMEN

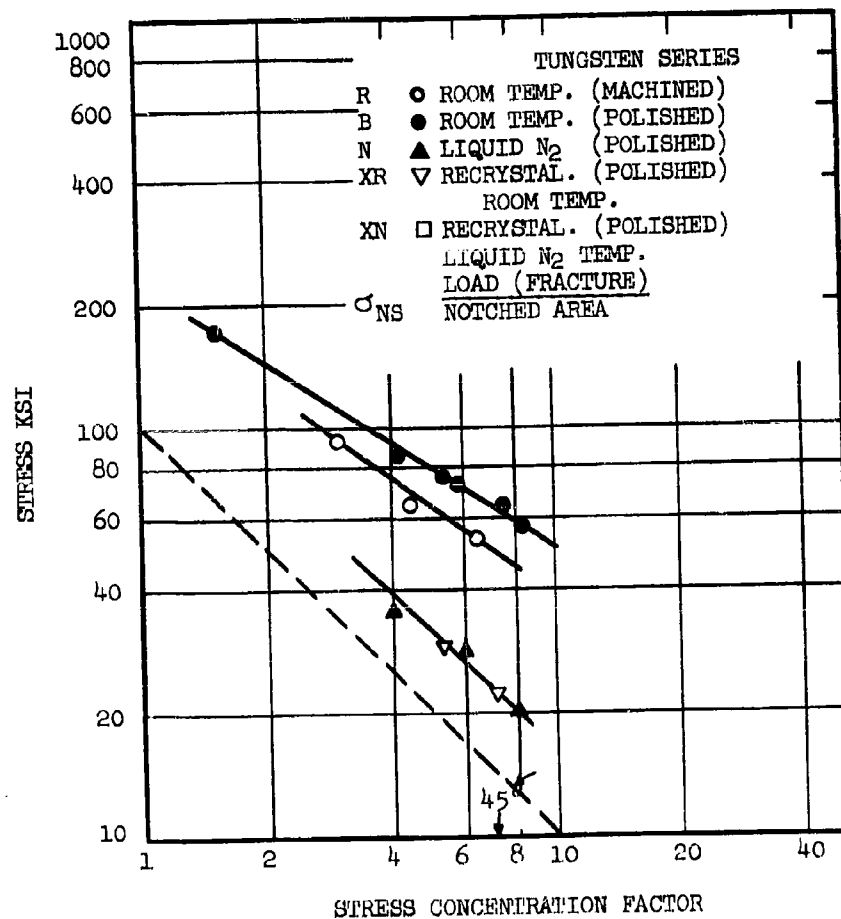FIG. 5b   REDESIGNED TEST SPECIMEN AND SPECIMEN HOLDER

FIG. 6 EFFECT OF STRESS CONCENTRATION FACTOR ON THE
NOTCH STRENGTH OF TUNGSTEN AT ROOM TEMPERATURE
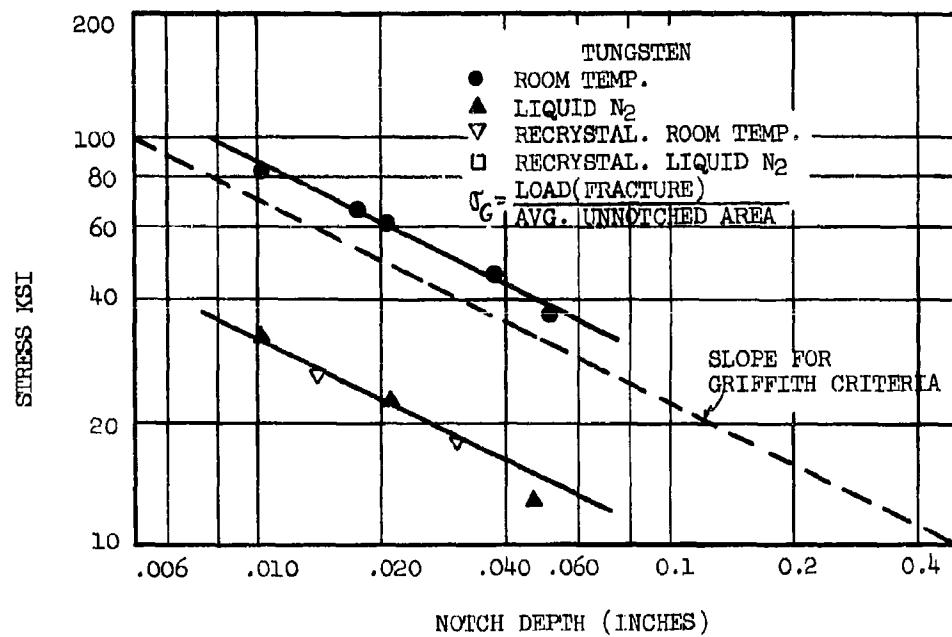AND CRYOGENIC TEMPERATURE.

FIG. 7   EFFECT OF NOTCH DEPTH ON AVERAGE STRESS ACROSS
UNNOTCHED SECTION AT ROOM AND LIQUID NITROGEN
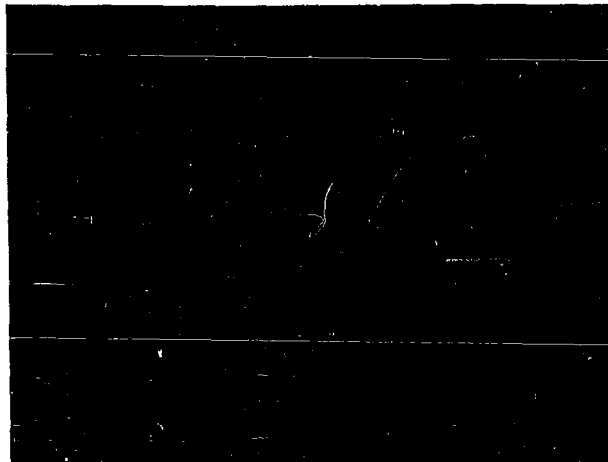TEMPERATURES ($r \cong .003'' - .004''$).

FIG. 8 DISLOCATION ARRAY IN AgCl SINGLE CRYSTAL. 500X ETCHED
IN KCN SOLUTION 1 MIN.

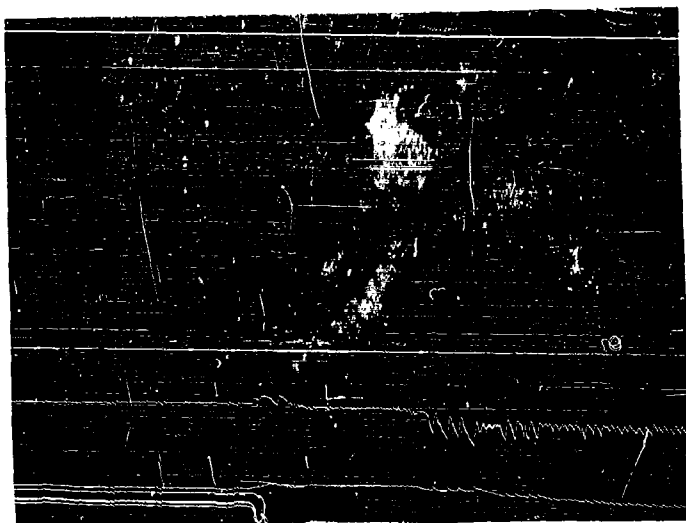FIG. 9 DISLOCATION ARRAY IN LiF SINGLE CRYSTAL. 1000 ETCH W 30 SEC.

FIG. 10 TIP OF CLEAVAGE CRACK IN LiF (100 SURFACE). 600X ETCH W
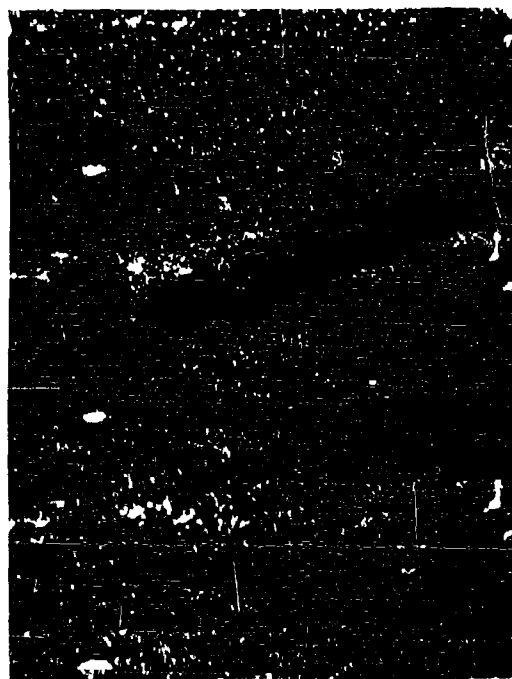10 SECONDS. PLANE OF CRACK IS (110).

FIG. 11 TIP OF CLEAVAGE CRACK IN LiF SIMILAR TO ABOVE. ETCH W
1 MIN. TO OUTLINE DISLOCATION DISTRIBUTION.

REFERENCES

1. G. Irwin, "Fracture", Handbuch der Physik, Springer, Berlin (Germany), Vol. 6, p. 551, (1958).

2. V. Weiss, "Current Views and Theories on Fracture, Crack Initiation and Propagation", Seventh Sagamore Ordnance Materials Research Conference, Syracuse University (1960).

3. H. Neuber, "Kerbspannungslehre", Springer-Verlag (1958).

4. A. A. Griffith   Phil. Transactions, Vol. 221 p. 163 (1921)

5. J. F. Hardrath and L. Ohman, "A Study of Elastic and Plastic Stress Concentration Factors Due to Notches and Fillets in Flat Plates", NACA TN 2566 (1951).

6. K. Grewal. V. Weiss, G. Sachs, J. Sessler, "A Study of Plastic Deformation in Flat Notch Specimens As a Function of Stress Level and Initial K_t," Syracuse University Met.E 604-6012FII for B.N.W. (1960).

7. V. Weiss, J. Sessler, K. Grewal, "The Effect of Stress Gradient and Stress Biaxiality on the Behavior of Materials", A.S.D.T.R. 61-725.

8. V. Weiss, J. Sessler and G. Sachs, "Analysis of Brittle Fracture in Sheet Materials", Symposium on Design with Materials that Exhibit Brittle Behavior, Materials Advisory Board (1960).

9. G. B. Espey, M. H. Jones, W. F. Brown, Jr., "The Sharp Edge Notch Tensile Strength of Several High Strength Sheet Alloys", Proc. ASTM Vol. 59 p. 837 (1959).

10. G. Sachs, J. Sessler, "Effect of Stress Concentration on Tensile Strength of Titanium Steel Alloy Sheet at Various Temperatures", ASTM STP 287 ASTM p. 122 (1960).

11. G. Gerard, N. Papirno, "Ductility Ratio of Aged Beta Titanium Alloy", ASTM Quarterly Sept. 1962 p. 373.

12. V. Weiss, Discussion to ref. (11) to be published ASTM Quarterly.

13. P. Packman, "Effect of Stress Gradient on Fracture", Master's Thesis Syracuse University (1961).

14. K. Loetsch, "Contribution to the Mechanics of Stresses During Constrained Deformation", Oesterr. Ingenieur Archiv Vol. 13 p. 191 (1959).

15. G. Irwin, et al, "Fracture Testing of High Strength Sheet Materials ASTM Special Pub. p. 29 (1960).

16. M. Metzger, Rev. of Sci Inst. Vol. 29 p. 620 (1958).

17. J. W. Mitchell, Dislocations of Crystals of Silver Halides in "Dislocations and Mechanical Properties of Crystals", John Wiley and Sons, New York p. 69 (1956).

18. J. J. Gilman and W. G. Johnston, "The Origin and Growth of Glide Bands in LiF Crystals", op. cit. John Wiley and Sons, New York p. 116 (1956).

19. J. J. Gilman, and W. G. Johnston, J. App. Phys. Vol. 27 p. 1 (1956)

20. J. J. Gilman, J. Metals Trans AIME Vol. 209 p. 449 (1957).

21. V. Weiss, "Application of Weibull's Statistical Theory of Fracture to Sheet Specimens", ASME Preprint 62-WA270 (1962).

APPENDIX I

THE EFFECT OF SURFACE STRUCTURE ON THE BRITTLE
FRACTURE STRENGTH OF METALS

Klaus Schroder

ABSTRACT

The theoretical fracture strength for brittle material
(approximately 0.1 E) has been reached for certain glass fibers and
some metal whiskers. However, metals with very high fracture strengths,
such as hard drawn steel springs or pure copper, deformed at liquid He
temperatures break at about one tenth of this value. A possible
explanation of some of the observed fracture stresses is presented
which is based on the effect of super-imposed stress concentration
fields. It seems possible that small surface slip steps could give

factor being of the order of 4 to 40 and thus the theoretical fracture
strength is reduced by this factor. Only metals without slip steps
can reach the theoretical fracture strength.

I

I. INTRODUCTION

The theoretical brittle fracture strength , which is approximately equal to

$$\sigma_M \simeq \sqrt{\frac{E\gamma}{a}} \simeq \frac{E}{10}$$

(Griffith, 1921; Cottrell, 1959) (E = Modulus of elasticity,

γ = specific surface energy, a = atomic spacing) has been obtained only in a few experiments with glass fibers and metal whiskers (Herring and Galt, 1952; Webb and Forgeng, 1958) while in other cases only a fraction of this strength σ_M has been attained. An attempt to explain some of these experimental results with the assumption that small surface slip steps act as stress raisers will be made.

Extensive investigations on mechanically and electrolytically polished surfaces have shown that plastic deformation is associated with the development of a microstructure on a smooth surface. Light microscopy on single crystals indicated that there are characteristic differences in the surface structure of cubic and hexagonal metals (Kuhlmann, 1950; Staubwasser, 1959; Diehl, 1956; Masing and Schröder, 1955).

Real progress in the interpretation of surface phenomena has been made by using electron microscopy. Correlation of electron micrographs with stress-strain curves of single crystals made it possible to interpret in detail observed slip lines, slip bands, cross slip etc. with the movement of screw and edge dislocations on regular slip planes, and cross slip on other crystallographic planes. It was also possible to obtain a more detailed model of the operation of dislocation sources (Seeger, 1958).

II

A typical surface structure as obtained from electron micrographs on aluminum is given in Fig. 1 (Seeger, 1958), which was obtained by Wilsdorf and Kuhlmann-Wilsdorf (1952). Plastic deformation produces steps with a height of 50 to 500Å. The step width has dimensions of the same order of magnitude. Several steps form a slip band, which corresponds frequently to one slipline as observed with a light microscope. Investigations at low temperatures indicate a decrease in the number of steps with decreasing temperature, but a complete interpretation of surface pictures has not been possible because of lack of resolution (Brown, 1950; Diehl, Mader and Seeger, 1955; Noggle and Koehler, 1951; Müller and Leibfried, 1955). Studies on copper single crystals have shown that the surface structure at low stresses is rather uniform (Mader, 1957). Deformation in the "easy glide" region causes surface steps usually 12 Burgers vectors high, i.e. about 12 edge dislocations leave the lattice in one plane. Further deformation does not appear to increase the step height, but to activate other slip planes. This changes when the stress increases more rapidly with strain because a critical internal stress concentration has been reached and slip in secondary starts (Schröder, 1959). The distance of the slip steps is about 400Å at the end of "easy glide".

Complications arise for alloys. For instance, it has not been decided if the high slip steps in α brass are due to slip on one plane, as Suzuki and Fujita (1954) suggested, or if multiple slip occurs on parallel glid planes close to each other. Wilsdorf and Flourie (1956) used five different methods to investigate this problem.

III

They came to the conclusion that slip is inhomogeneous and several parallel
slip planes are operating. Thus alloys may have the same surface structure
as the pure metal, as Wilsdorf and Kuhlman-Wilsdorf (1954) observed on
Al-Cu alloys, or the deformation is inhomogeneous as in ∝ brass.

II. STRESS CONCENTRATION AT SLIP STEPS

Mader (1957) found experimentally, as mentioned above, that the step height of slip steps does not increase continually in the region of "easy glide", but that steps of the same height are produced successively in different surface areas. This indicates a discontinuous supply of dislocations, and one would therefore expect, that the volume immediately behind the surface near the slip step is probably free of dislocations. There is a practically perfect lattice in the volume behind the step. It seems therefore appropriate to use the continuum theory of elasticity in such an area as a first approximation for the calculation of the stress distribution. The theory of elasticity shows that geometrical irregularities at the surface produce stress concentrations. Neuber (1958) showed that the stress concentration factor for shallow notches is $K = 1 + 2\sqrt{t/R}$ (t is the notch depth and R the notch root radius). An analytic expression for the stress concentration factor (SCF) of steps does not exist, but stress measurements, (Frocht, 1935; Frocht and Landsberg, 1951) indicate that the SCF of fillets is of the same order of magnitude as the SCF of notches. Therefore, it seems to be justified to assume that the SCF near the root of a slip step is of the order of $\sqrt{t''/R''}$, were t" is the slip step height and R" the radius at the root of the slip step. At the moment it is not possible to calculate or measure R", but it seems plausible to assume $R'' \simeq 1\overset{\circ}{A}$. t" could have values from twenty to several thousand Angstroms. It follows that the stress concentration factor K" is of the order of 4 to 50 assuming the validity of a maximum fracture stress concept (Weiss, Sessler, and Sachs, 1960; Weiss, 1960).

A metal with active slip planes can reach a maximum fracture strength of
only σ_M'

1)
$$\sigma_M' = \frac{\sigma_M}{K''} \leq \frac{E}{40}$$

where a theoretical strength of E/10 and a minimum K'' of 4 is assumed.
Only metals with a dislocation structure, which prevents the formation of
slip steps, can reach the theoretical fracture strength σ_M . This is the
case for metal whiskers, which have only one central screw dislocation.

III. FRACTURE STRENGTH OF NOTCHED SPECIMENS

A. Electrolytically Cut Notches

Experimental evidence indicates that the critical fracture strength of electrolytically cut notches is much higher than found in machined notches. Sessler and Sachs (1960) found that the extrapolated fracture strength in machined specimen with a composition of Ti-2.5Al-16V is about 200 ksi. Experiments on specimens of the same composition and heat treatment (solution treated and aged for 4 hours at 700°F) gave an extrapolated calculated maximum fracture stress at the notch root of more than 650ksi, if notches were cut with an electrolytic saw (Fig. 2).

It is proposed that this can be explained with the assumption of surface irregularities on machined notches which can act as stress raisers. A schematic picture of an electrolytically cut notch with slip steps is given in Fig. 3. The stress distribution, according to Neubers' Theory, is given schematically as a dash line in Fig. 3a. The stress at the root of the notch is given by the equation $\sigma'' = K'\sigma'$ where K' is the stress concentration factor and σ' the average stress in the notched section. The stress gradient at the root of the notch is given by

$$2) \qquad \frac{d\sigma''}{dy}\bigg|_{y=0} = \frac{2 K'\sigma'}{R'}$$

The stress reaches a hypothetical value of zero at a distance of R'/2 from the base of the notch, if a linear decrease in σ'' is assumed.

It is usually very difficult to make R' smaller than 10^{-2}cm. The stress in a volume element adjacent to the root of the notch with dimensions of the order of 10^{-4}cm is therefore practically constant if there are no further surface irregularities. Fig. 3b gives an idealized

VII

microscopic model of the root of the notch. Several dislocations left the specimen in one plane and formed a surface step with the length t". t" is, as mentioned above, approximately 10^{-7} to 10^{-5}cm. Dislocation densities in metals are of the order of 10^8 to 10^{12}cm^{-2}. The average dislocation distance "T" should therefore be of the order of 10^{-4} to 10^{-6}cm, and it is therefore assumed that dislocations be this distance away from the surface. The stress at A in Fig. 3b should be $\sigma_A = K''\sigma''$. It seems plausible to assume that the radius at A is of the order of one Angstrom. Therefore, the stress drops rapidly from the slip step to the center of the specimen and we have at B a stress practically equal to σ''. The specimen will fracture elastically at A, if the stress $\tilde{\sigma}_A \sim \tilde{\sigma}_M$ and if the dislocation at B does not move to relief the stress at A.

B. Machined Notches

We consider a system in which a notch with the radius R and the depth t is machined into the specimen. Small grooves are scratched during machining into the surface of the notch. Fig. 4a gives a schematic picture of such a notch with grooves of depth t' and radius R'. It will be assumed that the surface of the groove is smooth, so that only unavoidable slip step steps will produce stress raisers. In other words, the groove geometry is approximately the same as in an electrolytic notch as given in Fig. 3a and 3b. This assumption is certainly an oversimplification, but it is believed that the problems of superimposed geometric stress raisers can be adequately described with such a simple model, and that the principle in this argument can be applied to more complicated crack configurations. Effects of work hardening on the surface, of surface oxide films, etc. are neglected. It is assumed that the slip step in a groove has a radius R"

and the depth t". We will make the assumption that

$$3) \qquad R'' \ll R' < R \;, \qquad t'' \ll R' \;, \quad t' \ll R$$

These conditions are usually fulfilled. It is very difficult to machine notch radii R which are smaller than 10^{-2}cm. Typical values of dimensions of surface scratches t' and R' are 10^{-3} to 10^{-4}cm. Again, this is much larger than t", which is 10^{-5} to 10^{-7}cm, and R", which is approximately 10^{-8}cm. The calculations of the stresses are analog to the preceeding paragraph. The stress at the root of the notch will be given as $\sigma' = K \sigma$, (σ = average stress in notched cross section) and will be practically constant in the specimen to the depth of t', if there is no groove. A small groove with dimensions R' and t' will "see" only a stress $\sigma' = K \sigma$. Again using the theory of elasticity as given by Neuber, we have a stress concentration factor K' associated with this groove, and the stress at the root of groove is $\sigma'' = K' \sigma' = K K' \sigma$. The same arguments are used to calculate the stress acting on the root of the slip step. The radius of the groove R' is much larger than the length t" and the radius R" of the slip step, so that the stress field in the region of the step would have been practically constant without the step and equal to σ''. As pointed out above, such a step acts as a stress raiser with a SCF equal to K", so that again the elastic stress at A in Fig. 3b would be $\sigma_A' = K'' \sigma''$ Therefore, σ_A' is equal to

$$4) \qquad \sigma_A' = K'' \sigma'' = K'' K' K \sigma$$

if the stress fields can be superimposed.

The specimen will undergo brittle fracture at A if σ_M' is equal to $\sigma_M = \frac{E}{10}$. The log σ versus log K plot is preferred in the analysis of experimental measurements. The fracture condition for brittle fracture at the surface can therefore be written as:

5)
$$\log \sigma/(E/10) = -\log K'' - \log K' - \log K$$

K" is a property of the material. It can be changed by processes which influence the characteristics of the dislocation movement. K' depends on the properties of the machine tools and the material. Usually, grooves will not be separated. It is more likely that the surface of the notch is rather irregular as schematically given in Fig. 4b, but one should expect that there will be always some relatively deep grooves, which project from the irregular surface into the interior. They will be the principal stress raisers. K is given by the design of the specimen. The assumption that stress fields of various surface defects can be superimposed is not always justified. For instance, if the radius R decreases so much that it is of the same order of magnitude as t', it is not allowed to multiply K and K'. The stress gradient at the root of the notch would be so large that the stress at the root of the groove would be less than $K \sigma$. In the extreme case that R is only slightly larger than R'; or that t" is much larger than R, no stress raising is to be expected from the stress field of the notch, but only from the groove. Fig. 4c gives the model of a groove with depth t' protruding from a notch, where both the radius R and the depth t are much smaller than t'. Hence the stress at the root of the groove would be practically the same as if there would be no notch,

X

namely equal to K' δ which is always less than KK' δ . Therefore, the
experimentally observed log σ versus log K curve would not decrease linearly
with increasing K values, but would level as of schematically given in Fig. 5
because the true stress concentration factor is less than K K' K", and
a higher stress δ is hence necessary to start brittle fracture. Sessler
and Sachs (1960) measured log σ versus log K curves which show this
leveling off effect for large K values.

The theory of the effect of superimposed stress fields gives
similar results as the application of Neuber's theory of pointed notches
(1958) to brittle fracture by Sachs, Weiss and Sessler (1960). Neuber (1958)
derives an equation for the NSR of notches with very small radii. He assumes
that it is not allowed to integrate the elastic equations near the notch
root, because the stress field cannot be treated as homogeous. Neuber
shows then that the radius of the notch R in a specimen under simple
stress should be replaced by R + 2η , where η is the dimension in
which the classical theory is not applicable. An integration is not
allowed because finite increments should be used. It is easily seen
that for $R \rightarrow 0$ the effective SCF cannot increase to infinity, if SCF =
1 + 2 $\sqrt{t/(R + 2\eta)}$. The standard graph of log σ versus log K without the
use of η would level off. Neuber (1958) suggests no physical interpretation
of η . This can be given in the "multiple stress concentration" theory,
which predicts, as it was pointed out above, that the log σ versus log K
curve levels off, if the inequalities given in (3) are not applicable.
The stress concentration factors cannot be multiplied if the root radius
of the notch has the same order of magnitude as surface defects. Therefore,

X1

one could associate η with the dimensions of surface defects. It is obvious, that an integration of the elastic notch stress equation is then not justified.

IV. DISCUSSION

An investigation by Edmondson (see Allan, 1959) on the brittle fracture of iron single crystals, using temperature and orientation as parameters, showed that specimens become brittle with decreasing temperatures and with stress directions close to the $[100]$ direction. Fahrenhorst and Schmid (1932) found that the critical yield stress of iron single crystals does not vary significantly with orientation. Therefore, only the angle between $[100]$ direction and the stress axis and the relation between τ and σ_N (σ_N stress normal to fracture plane) should be important. One would therefore expect, as Allan (1959) pointed out, that cleavage dominates near the $[100]$direction. But it is surprising that one crystal close to the $[110]$ direction cleaves also, in spite of the fact that crystals closer to the $[100]$ direction are not brittle. Extensive investigations on strain hardening of single crystals indicate that the yield strength increases markedly if the crystal orientation favors multiple slip (Staubwasser, 1959; Lücke and Lange, 1952, 1953; Lücke, Masing and Schröder, 1955). This could also happen near the $[110]$ directions in iron. The yield strength is too high and brittle fracture starts. If this hypothesis is correct, cleavage should also be observed near the $[111]$ direction, but no experiments have been made with specimens of such orientation. Edmondson found in his experiments, that crystals which deformed plastically above the yield strength could be strained extensively. It is possible to have two crystals with orientations not more than 2° apart, where one fractures without measureable plastic deformation, while the other can be strained to more than 90% reduction in area.

XIII

This seems to be in contradiction to the model described above, because strain hardening increases the yield strength rapidly to the value needed for the initial brittle fracture. There may be several effects which could prevent brittle fracture after small amounts of plastic deformation, even if the stress increases rapidly due to strain hardening. For instance, the crystal orientation changes during deformation and the normal stress on the fracture plane decreases. It is probably more important that the surface structure changes. For instance new slip steps are produced. This could decrease the effective stress concentration at the root of the slip step, as Neuber proved for multiple notch systems.

On the other hand, fracture is quite frequently preceeded by small amounts of deformation, which produces slip steps on the surface. These slip steps are postulated to act as stress raisers which ultimately become the fracture nucleus.

V. SUMMARY

Some effects of the surface structure on the fracture characteristics of metals have been analyzed. It has been shown that slip lines will always lead to a reduction of the maximum surface fracture strength, and that the stress concentration factor associated with slip steps should be of the order from 4 to 50. An analysis of specific surface geometries showed that the stress concentration factors of various defects have in some cases, but not always, to be multiplied. It was possible to find a physical interpretation of the "finite particle dimension", previously used in the description of fracture properties of notches with a very small root radius.

ACKNOWLEDGMENT

REFERENCES

Allen, N.P.   1959   Fracture (J. Wiley & Sons) 123

Brown, A. F.   1950   Metallurgical Application of the Electron
                                Microscope (Inst. of Metals Monograph and
                                Report Ser. No. 8, London) 103

Cottrell, A.H.   1959   Fracture (J. Wiley & Sons) 20

Diehl, J., Mader, S.
and Seeger, A.   1955   Z. f. Metallk. 46, 53

Diehl, J.   1956   Z. f. Metallk. 47, 331, 411

Edmondson, B.   1959   see ref.: Allen (1959)

Fahrenhorst, W. and
Schmid, E.   1932   Z. f. Physik 78, 383

Frocht, M. M.   1926   Trans ASME 26 No.2 p255

Frocht, M. M.   1935   Trans ASME 57 A -67

Frocht, M. M. and
Landsberg, D.   1951   Proc. SESA 8, 149

Griffith, A. A.   1921   Phil. Trans. Roy. Soc. A 221, 163

Herring, C. and
Galt, J. K.   1952   Phys. Rev. 85, 1060

Kuhlmann, D.   1950   Z. f. Metallk. 41, 129

Lücke, K. and Lange, H. 1952   Z. f. Metallk. 43, 55

Lücke, K. and Lange, H. 1953   Z. f. Metallk. 44, 183

Lücke, K., Masing, G.
and Schröder, K.   1955   Z. f. Metallk. 46, 792

Mader, S.   1957   Z. f. Physik 149, 73

Masing, G. and
Schröder, K.   1955   Z. f. Metallk. 46, 860

Metzger, M.   1958   Rev. of Scient. Instr. 29, 620

Müller, H. and
Leibfried, G.   1955   Z. f. Physik 142, 87

XVII

Neuber, H.   1958   Kerbspannungslehre (Springer, Berlin)

Noggle, T. S. and
Koehler, J. S.   1951   J. of Appl. Phys. 22, 53

Sachs, G. and
Sessler, J. G.   1960   ASTM STP 287,122

Schröder, K.   1959   Proc. Phys. Soc. London 73, 674

Seeger, A.   1958   Handbuch der Physik (Springer, Berlin)
                                            Vol VII, 2

Staubwasser, W.   1959   Acta Met. 7, 43

Suzuki, H. and
Fujita, F. E.   1954   J. Phys. Soc. Japan 9, 428

Webb, W. W. and
Forgeng, W. P.   1958   Acta Met. 6, 426

Weiss, V.   1960   Seventh Sagamore Ord. Materials Research
                                            Conf., Syracuse Univ.

Weiss, V. Sessler, J.G.
and Sachs, G.   1960   Symposium on Design with Materials that
                                            Exhibit Brittle Fracture, Materials
                                            Advisary Board

Wilsdorf, H. and
Kuhlmann-Wilsdorf, D. 1952   Z. ang. Phys. 4, 361, 418

Wilsdorf, H. and
Kuhlmann-Wilsdorf, D. 1955   Report on a Conference on Defects in
                                            Crystalline Solids in Bristol 1954
                                            (Phys. Soc. London) 175

Wilsdorf, H. and
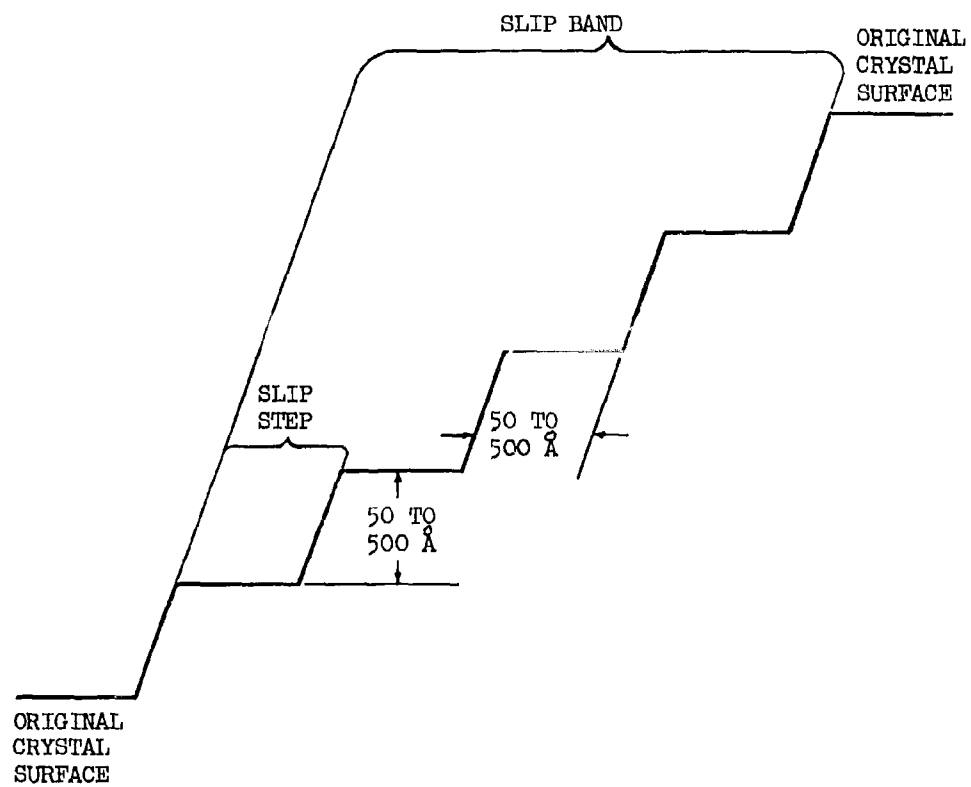Furie, J. T.   1956   Acta Met. 4, 271
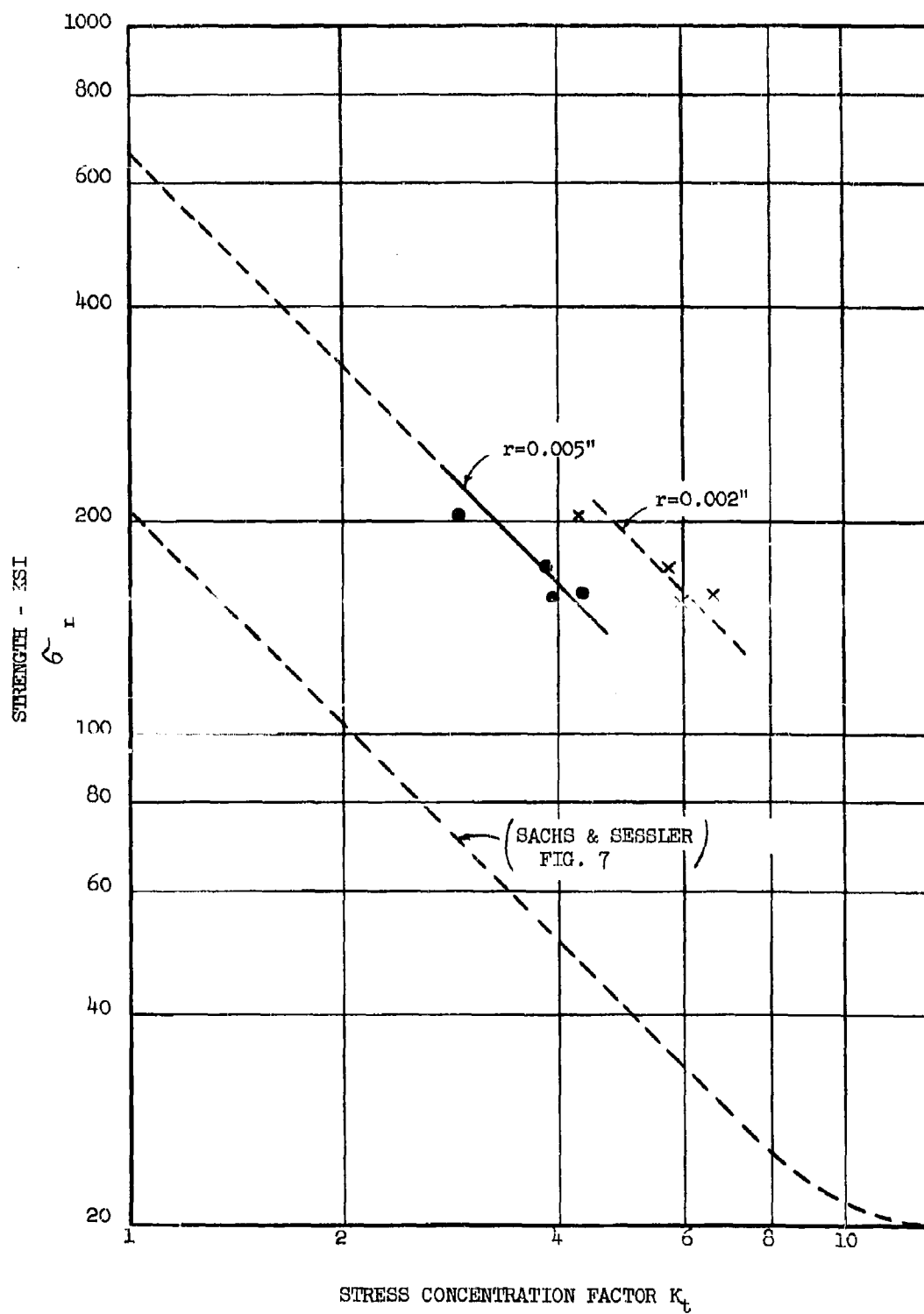
FIG. 1 SCHEMATIC PICTURE OF A GLIDE BAND

FIG. 2 NOTCH STRENGTH VERSUS STRESS CONCENTRATION FACTOR OF Ti - 2.5Al-16V, HEAT TREATED FOR MAXIMUM BRITTLENESS. NOTCHES PRODUCED WITH AN ELECTROLYTIC SAW.
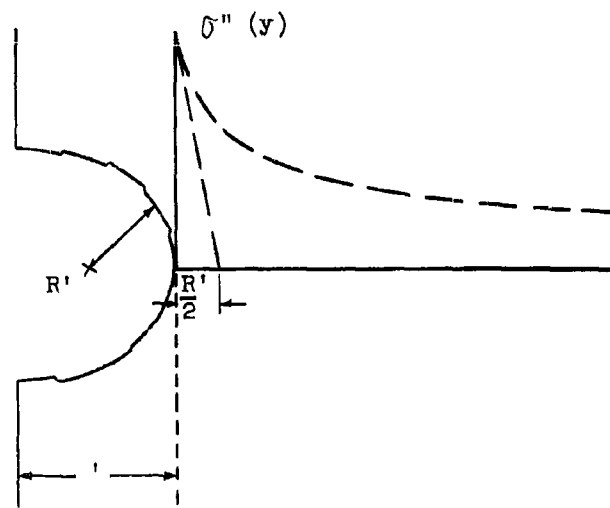
XX

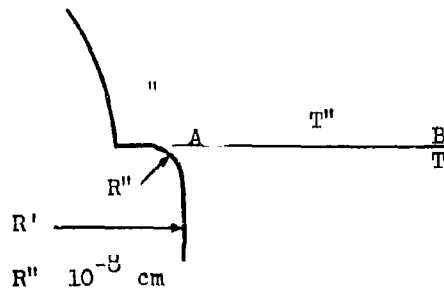FIG. 3a STRESS DISTRIBUTION AT THE ROOT OF AN ELECTROPOLISHED NOTCH
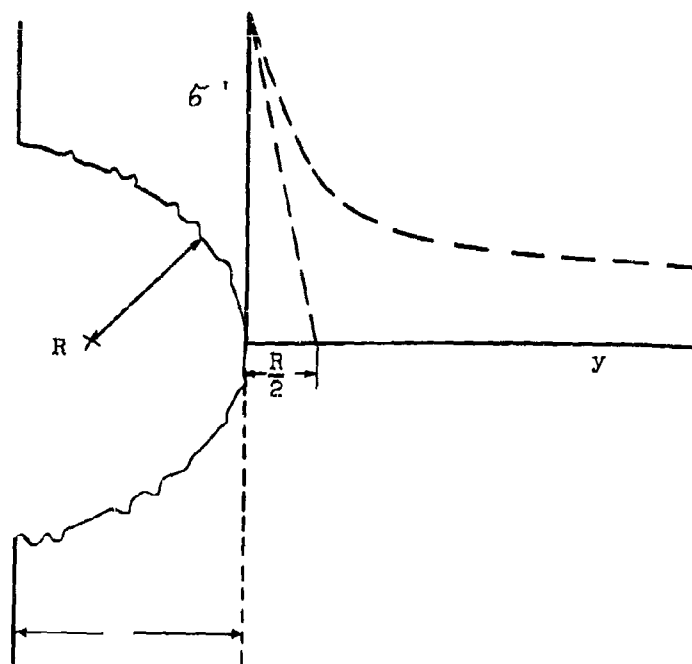

FIG. 3b STRESS DISTRIBUTION NEAR SLIP STEP

FIG. 4a STRESS DISTRIBUTION σ' AT THE ROOT OF A NOTCH
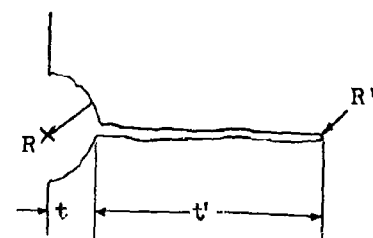

FIG. 4b SURFACE STRUCTURE OF
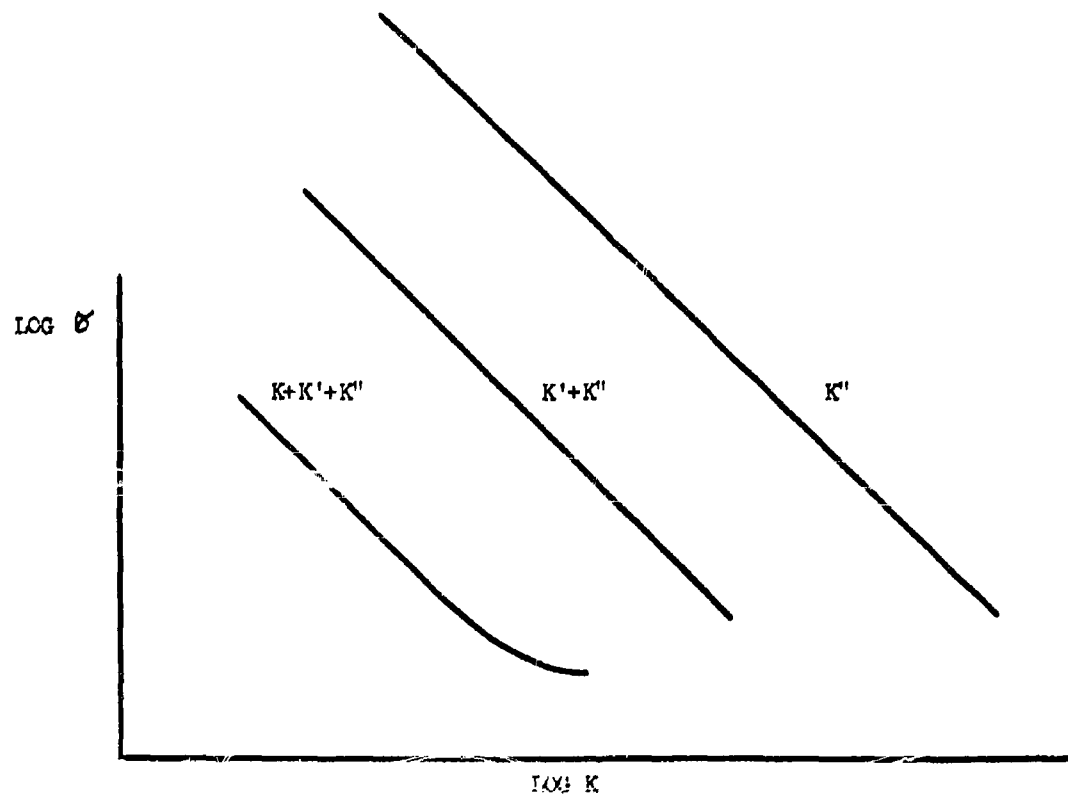A NOTCH

FIG. 4c DEEP CRACK AT ROOT
OF NOTCH

XXII

FIG. 5 MAXIMUM FRACTURE STRENGTH OF BRITTLE MATERIAL